JB
Journals.ASM.org

Characterization of BreR Interaction with the Bile Response Promoters *breAB* and *breR* in *Vibrio cholerae*

Francisca A. Cerda-Maira,[a] Gabriela Kovacikova,[a] Brooke A. Jude,[b] Karen Skorupski,[a] Ronald K. Taylor[a]

Department of Microbiology and Immunology, Geisel School of Medicine at Dartmouth, Hanover, New Hampshire, USA[a]; Biology Program, Bard College, Annandale-on-Hudson, New York, USA[b]

The *Vibrio cholerae* BreR protein is a transcriptional repressor of the *breAB* efflux system operon, which encodes proteins involved in bile resistance. In a previous study (F. A. Cerda-Maira, C. S. Ringelberg, and R. K. Taylor, J. Bacteriol. 190:7441–7452, 2008), we used gel mobility shift assays to determine that BreR binds at two independent binding sites at the *breAB* promoter and a single site at its own promoter. Here it is shown, by DNase I footprinting and site-directed mutagenesis, that BreR is able to bind at a distal and a proximal site in the *breAB* promoter. However, only one of these sites, the proximal 29-bp site, is necessary for BreR-mediated transcriptional repression of *breAB* expression. In addition, it was determined that BreR represses its own expression by recognizing a 28-bp site at the *breR* promoter. These sites comprise regions of dyad symmetry within which residues critical for BreR function could be identified. The BreR consensus sequence AANGTANAC-N_6-GTNTACNTT overlaps the −35 region at both promoters, implying that the repression of gene expression is achieved by interfering with RNA polymerase binding at these promoters.

Vibrio cholerae is a Gram-negative bacterium that causes the severe diarrheal disease cholera and is acquired by oral ingestion of contaminated water or food. Upon infection, the bacteria colonize the intestinal epithelium via the toxin coregulated pilus (TCP) and produce cholera toxin (CT), which induces severe loss of fluid and ions. A virulence regulatory system coordinately controls the production of a number of virulence factors, including CT and TCP. ToxT, a member of the AraC family of transcriptional regulators, is the direct activator of the genes encoding CT and TCP (1, 2). Expression of *toxT* is dependent upon a complex transcriptional regulatory cascade (3, 4).

During the course of infection, enteric pathogens encounter different environments within the stomach and the intestinal lumen, including changes in pH, CO_2, and osmolarity and the presence of bile (5). Bile is produced by the liver and stored in the gallbladder. It is secreted into the proximal portion of the duodenum upon ingestion of food. The main components of bile are bile salts, which are detergents that aid in the emulsification of dietary fats and in their absorption (6). Additionally, the detergent property of the bile salts affects the cell membrane of bacteria, acting in a bactericidal manner (5, 6).

Enteric bacteria, including *V. cholerae*, are able to employ bile as a host signal to modulate gene expression and overcome the bactericidal effect of bile (5, 7). *V. cholerae* resistance to bile depends on (i) increased motility in the presence of bile, which is hypothesized to be essential for evading the high concentrations of bile in the lumen, penetrating the mucus layer, and achieving access to the underlying epithelial cells for colonization (8, 9); (ii) biofilm formation, where cells inside the biofilm are resistant to the bactericidal effect of bile (10); (iii) selectively excluding bile from entering the cell by differentially expressing genes encoding the OmpU and OmpT porins (11–13); and (iv) extruding bile out of the cell by inducing the expression of genes encoding proteins involved in efflux, such as *acrA* (14), *tolC* (15), *vceB* (16), *vexB* (11), and *breB* (11, 17).

We have recently demonstrated that the expression of *breB*, encoding an efflux pump belonging to the RND family, is induced by bile and bile salts (cholate, deoxycholate, and chenodeoxycholate) (17). The expression of genes encoding multidrug transporters is usually tightly controlled by transcriptional regulators to prevent nonspecific transport and loss of membrane potential that could result in cell death (18, 19). We have established that BreR, a member of the TetR family of transcriptional regulators, is a direct repressor of *breAB* operon expression, and that it binds at two independent sites at this promoter (17). Typically, genes encoding TetR repressors that control the expression of genes encoding efflux pumps are located either in the same operon or adjacent and are divergently transcribed from the genes they regulate (20–25). However, the *breR* gene is located 8.99 kb upstream of the *breAB* operon, with several genes between them. Like other TetR regulators, BreR is able to regulate its own expression (negative regulation), and it binds to a single site at the *breR* promoter (17). Furthermore, *breR* expression is induced in the presence of bile, cholate, deoxycholate, and chenodeoxycholate, and it has been shown that deoxycholate prevents BreR binding to the *breR* promoter (17).

The present study examines BreR binding sites and their locations in the *breR* and *breAB* promoter regions to gain a better understanding of the mechanism of BreR-mediated repression. Electrophoretic mobility shift assays (EMSA) and DNase I footprinting demonstrate that BreR recognizes a single 28-bp binding site at its own promoter (−51 to −24) and two binding sites at the *breAB* promoter separated by 141 bp, a 29-bp proximal binding site (−54 to −26), and a 29-bp distal binding site (−224 to −196). Transcriptional assays showed that the mutations at the *breR* promoter resulted in P_{breR}-*lacZ* overexpression, and EMSAs confirmed that the mutations prevented BreR from binding. However, only mutations at the proximal site at the *breAB* promoter

Received 29 October 2012 **Accepted** 1 November 2012
Published ahead of print 9 November 2012
Address correspondence to Ronald K. Taylor, ronald.k.taylor@dartmouth.edu.

doi:10.1128/JB.02008-12

TABLE 1 Bacterial strains and plasmids used in this study

Strain or plasmid	Relevant genotype	Source or reference
Vibrio cholerae strains		
C6706 str2	E1 Tor Sm^r	Laboratory collection
KSK262	C6706 str2 Δ*lacZ3*	3
FCM274	KSK262 Δ*breR1*	This work
FCM158	KSK262 P_{breR}-*lacZ1*	17
FCM191	FCM158 Δ*breR1*	17
FCM313	KSK262 P_{breR}-*lacZ1* A-50G/A-44G	This work
FCM315	FCM274 P_{breR}-*lacZ1* A-50G/A-44G	This work
FCM345	KSK262 P_{breAB}-*lacZ1*	This work
FCM321	FCM274 P_{breAB}-*lacZ1*	This work
FCM291	KSK262 P_{breAB}-*lacZ1* A-223G/T-220C/A-217G	This work
FCM293	FCM274 P_{breAB}-*lacZ1* A-223G/T-220C/A-217G	This work
FCM295	KSK262 P_{breAB}-*lacZ1* A-52G/T-49C/A-46G	This work
FCM297	FCM274 P_{breAB}-*lacZ1* A-52G/T-49C/A-46G	This work
FCM301	KSK262 P_{breAB}-*lacZ1* A-223G/T-220C/A-217G A-52G/T-49C/A-46G	This work
FCM303	FCM274 P_{breAB}-*lacZ1* A-223G/T-220C/A-217G A-52G/T-49C/A-46G	This work
Plasmids		
pKAS154	pKAS32 derivative, Kan^r	27
pGKK346	*lacZ* in pGKK344	17
pFC3	pKAS154, Δ*braR1*	This work
pFC31	pKAS154, 235 bp harboring the R site	This work
pFC29	pKAS154, 230 bp harboring the AB_d site	This work
pFC30	pKAS154, 246 bp harboring the AB_p site	This work
pFC27	P_{breR}-*lacZ1* in pGKK346	This work
pFC42	P_{breR}-*lacZ1* A-50G/A-44G in pGKK346	This work
pFC43	P_{breAB}-*lacZ1* in pGKK346	This work
pFC38	P_{breAB}-*lacZ1* A-223G/T-220C/A-217G in pGKK346	This work
pFC39	P_{breAB}-*lacZ1* A-52G/T-49C/A-46G in pGKK346	This work
pFC40	P_{breAB}-*lacZ1* A-223G/T-220C/A-217G A-52G/T-49C/A-46G in pGKK346 pFC42	This work

caused P_{breAB}-*lacZ* overexpression and loss of BreR binding by EMSA. The distal binding site did not exhibit any regulatory role *in vivo*. Altogether, these results indicate that the BreR binding sites overlap the −35 regions of the *breAB* and *breR* promoters, suggesting that BreR inhibits initiation of transcription by blocking RNA polymerase access to the promoter sequences.

MATERIALS AND METHODS

Bacterial strains, plasmids, primers, and growth conditions. The *V. cholerae* strains, plasmids, and primers used in this study are listed in Tables 1 and 2. The strains were grown in Luria-Bertani (LB) medium (26). Antibiotics (Sigma) were used at the following concentrations: kanamycin, 45 μg/ml; polymyxin B, 50 U/ml; and streptomycin, 100 μg/ml or 1 mg/ml (allelic exchange experiments). For P_{breR}-*lacZ* and P_{breAB}-*lacZ* induction experiments, strains were grown in subinhibitory concentrations of sodium cholate (crude bile; Sigma) as noted in the β-galactosidase assay methods. Bile stocks were freshly prepared in LB medium and filter sterilized. For allelic exchange experiments, LB agar contained 40 μg/ml 5-bromo-4-chloro-3-indolyl-β-D-galactopyranoside (X-Gal; Gold Biotechnology Inc.).

Construction of in-frame deletion strains. The deletions were obtained by PCR amplifying, from C6706 str2, ~500-bp DNA fragments flanking the gene of interest while retaining several codons from the 5′ and 3′ ends of the gene fused in frame. The fragments were ligated into pKAS154 (27), and the different genes were deleted from the *V. cholerae* chromosome by allelic exchange (28). The deletion of *breR* was obtained using TR3B with TR3N2 and TR3N1 with TR3E. The constructs were confirmed by DNA sequencing.

Construction of the P_{breAB}-*lacZ* fusion. The pGKK346 plasmid was linearized with XbaI between the chromate homology fragment and the promoterless *lacZ* gene (17). Approximately 500 bp of the *breAB* promoter region was amplified by PCR using FC70 with FC71. The resulting fragment was digested with XbaI and ligated into the linearized pGKK346 plasmid, generating pFC43. The *lacZ* fusions were transferred into the chromosome of a *V. cholerae* Δ*lacZ* strain by allelic exchange (28) between the *chr* and *gal* loci. All of the constructs were confirmed by DNA sequencing.

Introduction of base pair changes into the P_{breR}-*lacZ* and P_{breAB}-*lacZ* fusions. The mutations were introduced into the R, the $AB_{proximal}$ (AB_p), and the AB_{distal} (AB_d) binding sites by PCR amplifying fragments from C6706 str2 using overlapping primers containing the site for the SapI enzyme. The A-50G/A-44G changes in the R binding site were obtained using FC68 with FCmut11-Sap and FC69 with FCmut2-Sap. The A-52G/T-49C/A-46G changes in the AB_p binding site were obtained using FC70 with FCmut5-Sap and FC71 with FCmut6-Sap, and the A-223G/T-220C/A-217G changes in the AB_d binding site were obtained using FC70 with FCmut3-Sap and FC71 with FCmut4-Sap. The resulting fragments were then digested with XbaI and SapI and ligated into a linearized (XbaI) pGKK346 plasmid, generating pFC38 (AB_d mutations), pFC39 (AB_p mutations), and pFC42 (R mutations). The double AB_d and AB_p mutations were obtained by PCR amplifying fragments from pFC38 using FC71 with FCmut6-Sap and FC70 with FCmut5-Sap. The fragments were digested with XbaI and SapI and ligated into a linearized (XbaI) pGKK346, generating pFC40. After screening for the correct orientation of the fragment, the *lacZ* fusions were transferred into the chromosome of a *V. cholerae* Δ*lacZ* strain by allelic exchange between the *chr* and *gal* loci. All of the constructs were confirmed by DNA sequencing.

TABLE 2 Primers used in this study

Name	Nucleotide sequence (5′ to 3′)
FC13F	GATCGGGATCCCGTAAGCAATCTCGCTACTG
FC18F	GATCGGAATTCACCATGAAACTCAGTGAGCAAAA
FC24	AGCAGACACTCAGATTATCG
FC25	CGATAATCTGAGTGTCTGCT
FC26	TGTACGAATCCCCATGCCTT
FC27	GTGGTTAACTTGTCGCGCAT
FC30	GATTTAATGGTGTCTACACG
FC31	AGGTGCCGCTCAAAGATACG
FC35	GCACAAAGTAAACTCGTTGG
FC36	GCTTTCTCCTTTTGGGTTGAGCAG
FC37	CTTGAGTAATGATAAAAAGTAAAC
FC39	GGCGATAATACCTTTATTTTTAG
FC40	CGTTGGTGTACTTTTTTGTGCGTCG
FC41	TTTTGCTCACTGAGTTTCAT
FC42F	GATCGGGATCCAGCACTGGAAACTACAGGTAAG
FC42R	GATCGGAATTCAGCGAGTTACCAATTGGGTTTCG
FC43F	GATCGGGATCCTCTGGTTGAAGCACTCTCTG
FC43R	GATCGGAATTCGTACGAATCCCCATGCCTTTG
FC44F	GATCGGGATCCGCTTCAATCAGCGCCAACCG
FC44R	GATCGGAATTCATACTTGGGGAGCAATGAATCTG
FC45	TCTTGGTTTAACATGCTTTCTCC
FC46	CGTATCTTTGAGCGGCACCTG
FC47	CTTTCGGGTGTACATTTGTG
FC48	GAACTGCTCAACCCAAAAGG
FC68	GATCGTCTAGACGATTGAATCGACGTTGATCCCTTG
FC69	GATCGTCTAGAGATCCATATTCGCTGCATGG
FC70	GATCGTCTAGACGTAAGCAATCTCGCTACTG
FC71	GATCGTCTAGAGAAGGATTCATAGTGTGTTG
FC1DIG	/5DigN/CGTAAGCAATCTCGCTACTGGCCTGCACC TTTG
FC2DIG	/5DigN/CGATAATCTGAGTGTCTGCTCAGCGAGTTA
FC3DIG	/5DigN/AGCAGACACTCAGATTATCGATAGAATAAA
C4DIG	/5DigN/GAAGGATTCATAGTGTGTTGCTCCTCAATT
FC7DIG	/5DigN/TTTCTGATCCCTGAATGCCATTTTGAGGCG
FC8DIG	/5DigN/GATCCATATTCGCTGCATGGAATCCAA ACTG
FCmut2-Sap	GATCGGCTCTTCGCTCGTTGGTGTACTTTTTTG
FCmut3-Sap	GATCGGCTCTTCGGGTCTAGCACGCTTTCTCCTT TTGGGTTGAG
FCmut4-Sap	GATCGGCTCTTCGACCAAGAGTTTAGTTTTCAGG
FCmut5-Sap	GATCGGCTCTTCGGGGCGTGCACTTGTGTTGGG CTTTTTATTCTATCG
FCmut6-Sap	GATCGGCTCTTCGCCCGAAAGTTTACTTTTTATC ATTACTCAAG
FCmut11-Sap	GATCGGCTCTTCGGAGCTTACTCTGTGCTAAAA ATAAAGGTATTATCG
TR3B	GATCGGGATCCTAATCGCGGCAACCCAGCCAA
TR3E	GATCGGAATTCCGATTGAATCGACGTTGATCC
TR3N1	GATCGGCGGCCGCGATCCATATTCGCTGCATGGA
TR3N2	GATCGGCGGCCGCAAAGCCTTAGAGGCTAACGGAT

β-Galactosidase assays. Different *V. cholerae* strains harboring the wild-type or mutated P_{breR}-*lacZ* or P_{breAB}-*lacZ* transcriptional fusion were grown for 15 h in LB medium at 37°C with aeration. The cultures were then diluted 100-fold into LB medium with or without crude bile (0.4%) and were grown at 37°C with aeration until the OD_{600} of the culture had reached 0.8 to 1.0. β-Galactosidase assays were carried out as previously described (26).

EMSA. The R3, R4, R5, and R6 fragments were amplified from C6706 str2 using primers pairs FC35 and TR3N1, FC18F and TR3N1, FC39 and FC41, and FC40 and FC41, respectively. The AB3, AB4, AB5, AB6, AB7, AB8, AB9, AB10, AB11, and AB12 fragments were amplified from C6706 str2 using primer pairs FC30 and FC25, FC31 and FC25, FC13F and FC46, FC13F and FC45, FC13F and FC36, FC24 and FC26, FC24 and FC27, FC31 and FC37, FC31 and FC47, and FC48 and FC37, respectively. Following amplification, these fragments were 3′ end labeled with digoxigenin (DIG) as previously described (29). The wild-type R1, AB1, and AB2 fragments were amplified from C6706 str2 using the DIG-labeled primer pairs FC7DIG and FC8DIG, FC3DIG and FC4DIG, and FC1DIG and FC2DIG, respectively. The mutated R1, AB1, and AB2 fragments were amplified from pFC42, pFC39, and pFC38, respectively, using FC7DIG and FC8DIG, FC3DIG and FC4DIG, and FC1DIG and FC2DIG, respectively. All of the fragments, including those amplified with DIG-labeled primers, were gel purified as previously described (29). Binding reactions were performed using formerly purified BreR-His_6 (17) with different fragments in the presence of the nonspecific competitor poly(dI-dC), followed by electrophoresis in 6% polyacrylamide gels as previously described (22). The DNA was transferred, probed, and detected as previously described (30).

DNase I footprinting. DNA fragments for footprinting assays were amplified from C6706 str2 by PCR. A 230-bp fragment carrying the AB_d binding site was amplified using FC42F with FC42R, a 246-bp fragment harboring AB_p was amplified using FC43F with FC43R, and a 235-bp fragment containing the R binding site was amplified using FC44F with FC44R. These fragments were ligated into pBluescript (Stratagene), generating pFC29, pFC30, and pFC31, respectively. For coding strand labeling, the inserts were excised with XbaI and EcoRI. For noncoding strand labeling, the inserts were excised with BamHI and HindIII. The fragments were gel purified (Qiagen), treated with shrimp alkaline phosphatase (NEB), and then end labeled with [γ-^{33}P]ATP (3,000 Ci/mmol; NEN) using T4 polynucleotide kinase (Amersham Biosciences). Single end-labeled fragments were obtained by digestion with BamHI (coding strands) and EcoRI (noncoding strands). Binding reactions of BreR to the radiolabeled fragments were performed using the binding conditions defined above for EMSA. After incubation, the fragments were treated with various DNase I (Ambion) concentrations and loaded onto 6% acrylamide sequencing gels as previously described (29). The gels were dried and visualized by autoradiography.

Colonization assays. The infant mouse competition assays were performed essentially as previously described (31). Suckling CD-1 mice (3 to 5 days old; Charles River) were inoculated orally, and the total CFU were obtained from the small intestine of four to six mice after 24 h by plating intestinal homogenates on streptomycin X-Gal plates.

RESULTS

BreR binds to a single site between −55 and −24 in the *breR* promoter. To learn more about BreR regulation at the *breR* promoter, we sought to identify the DNA elements involved in BreR binding. Regulators belonging to the TetR family usually bind as homodimers to regions of complete or partial dyad symmetry (32). BreR was previously shown to bind to the *breR* promoter fragment R1 (−102 to 131) (17). In order to determine which region(s) of the *breR* promoter is critical for BreR binding, the R1 fragment was examined for the presence of regions of dyad symmetry using the Vienna RNA Secondary Structure Prediction program (http://rna.tbi.univie.ac.at/cgi-bin/RNAfold.cgi). Figure 1A shows, with arrows, putative regions of dyad symmetry in the R1 fragment (ds1, ds2, and ds3) as predicted by the Vienna program and in a size range typical of regulatory protein binding sites. Based on these predictions, we generated various fragments to delineate the minimal segments containing regions of dyad symmetry that are essential for BreR binding at the *breR* promoter (Fig. 1A).

To localize the BreR binding site at the *breR* promoter, EMSAs were performed using the R3 (−55 to +131), R4 (−77 to +60),

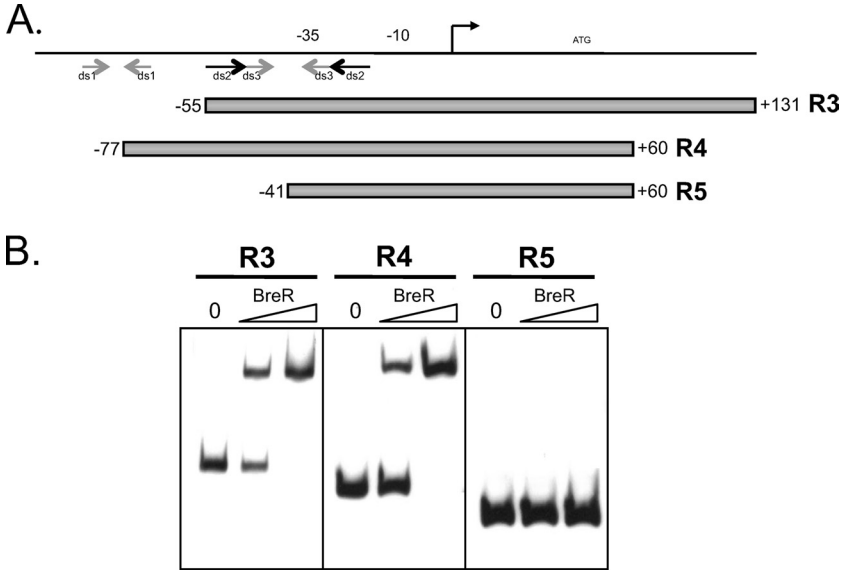

FIG 1 Mapping of the BreR binding site within the *breR* promoter region using EMSA and dyad symmetry prediction. (A) Schematic representation of the R1 fragment showing the regions of dyad symmetry predicted by the Vienna program. Putative regions of dyad symmetry (ds1, ds2, and ds3) are indicated by gray or black arrows. Various DNA fragments (R3, R4, and R5) used for EMSA are shown by gray boxes. The transcriptional start site is indicated by a black arrow. The ATG start codon and putative −35 and −10 regions are also shown. (B) EMSA showing BreR binding to *breR* promoter region fragments R3, R4, and R5. In each panel, 10 ng DIG-dUTP-labeled DNA was incubated with 0 (first lane), 50 (second lane) or 250 ng (third lane) of purified BreR-His_6 prior to electrophoresis.

and R5 (−41 to +60) fragments containing various regions of dyad symmetry (Fig. 1B). Increasing amounts of BreR caused a shift of the R3 and R4 fragments but not of the R5 fragment (Fig. 1B), indicating that the region from −55 to −41 containing the upstream halves of regions of dyad symmetry ds2 and ds3 is critical for BreR binding (Fig. 1).

DNase I footprinting analyses were performed to further localize the BreR binding site(s) in the *breR* promoter. BreR was incubated with a 235-bp radioactively labeled fragment extending from positions −158 to +81. This fragment showed a single region of strong protection, indicating that a single site is necessary for BreR protection at the *breR* promoter (Fig. 2A). On the coding strand, this site extended from positions −51 to −24 (Fig. 2A). On the noncoding strand, the protected region extended from −28 to −55 (Fig. 2A). Further examination of the protected region revealed the presence of a region of partial dyad symmetry (containing 2 mismatches) that consists of 9-bp half sites (Fig. 2B, indicated by gray arrows) separated by a 6-bp spacer. These results show that BreR DNase I protection overlaps both ds2 and ds3 regions of dyad symmetry and indicate that BreR directly represses *breR* expression by interacting with a binding site that overlaps the *breR* −35 region. The BreR binding site at the *breR* promoter will be referred to here as the R binding site.

BreR binds to a proximal (−56 and −26) and a distal (−228 to −196) site in the *breAB* promoter. In a previous study, a *breAB* promoter region (−382 to +131) utilized for the *lacZ* transcriptional fusions was divided into two fragments, an ~230-bp fragment named AB1 (−95 to +132) and an ~300-bp fragment named AB2 (−382 to −76) (17). It was shown by EMSA that BreR binds to the AB1 and AB2 fragments, indicating that BreR binds at two independent binding sites at the *breAB* promoter (17). To further define the binding sites for each of the individual fragments, a series of *breAB* promoter fragments (distal fragments included AB3 [−297 to −76], AB4 [−198 to −76], AB5 [−382 to −179], AB6 [−382 to −210], and AB7 [−382 to −224]; proximal fragments included AB8 [−95 to +79], AB9 [−95 to +10], AB10 [−198 to −15], and AB11 [−198 to −38]) were used in gel mobility shift assays with increasing amounts of purified BreR (Fig. 3A and B). For the distal region, BreR bound to AB3 and AB5 but not AB4, AB6, or AB7 (Fig. 3B). This suggests that a region from −210 to −179 is critical for binding. For the proximal region, we observed that BreR bound to AB8, AB9, and AB10 but not AB11 (Fig. 3B). This result indicates that a region from −38 to −15 is critical for binding. As a whole, these binding patterns suggest that the regions from −95 to −15, containing ds11 and ds12, and from −297 to −179, containing ds5, ds6, and ds7, are critical for BreR binding to the proximal and distal sites, respectively (Fig. 3A and B). These data confirm our previous findings and establish that in EMSAs BreR binds the *breAB* promoter at both a proximal (named AB_p) and a distal (named AB_d) site with respect to the +1 position. Additionally, we generated the AB12 fragment containing both the AB_p and the AB_d binding sites. When the AB12 fragment was incubated with BreR, a double shift was observed at a low BreR concentration (50 ng), with the lower band having a much greater intensity than the upper band (Fig. 3B, second lane). At a higher BreR concentration (250 ng), the intensity of the upper band was significantly increased (Fig. 3B, third lane), supporting the hypothesis that BreR recognizes two independent sites present at the *breAB* promoter.

DNase I footprinting was used to further map the BreR binding sites within the *breAB* promoter using a 230-bp (−327 to −97) and a 246-bp (−167 to +78) radioactively labeled fragment containing the individual AB_d and AB_p sites, respectively. BreR protected a single region from DNase I digestion on each fragment (Fig. 4A and B). The AB_d binding site extends from −224 to −196 and from −201 to −228 on the coding and noncoding strands,

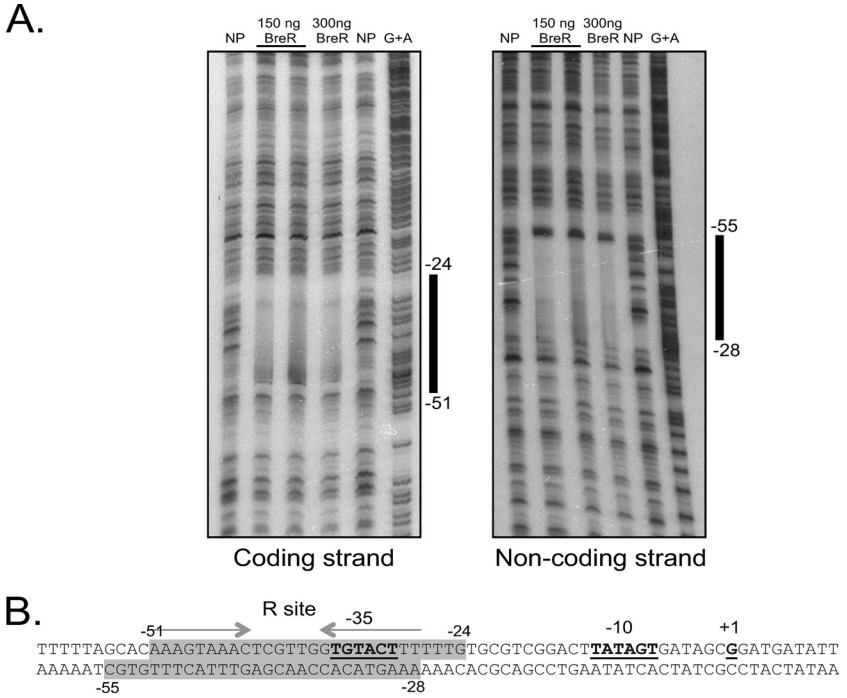

FIG 2 DNase I protection of the *breR* promoter by BreR. (A) The coding and noncoding strands of the ^{33}P-end-labeled fragment from positions −158 to +81 were incubated with a 1:200 dilution of DNase I and no protein (NP; lanes 1 and 5), ~150 ng BreR and a 1:200 DNase I dilution (lane 2) or a 1:400 DNase I dilution (lane 3), ~300 ng BreR and a 1:200 dilution of DNase I (lane 4), and a G+A sequencing reaction (lane 6). The region of protection by BreR is indicated with a black bar. (B) Double-stranded DNA sequence showing the BreR-protected region at the *breR* promoter. The protected region for both strands is shaded in gray, and the endpoints of the protection above and below the shaded regions are labeled (−55 to −24). A region with partial dyad symmetry, involved in DNA binding, is indicated by gray arrows. The transcriptional start site (+1) (17) and putative −35 and −10 regions are highlighted in boldface and are underlined.

respectively (Fig. 4A). DNase I hypersensitivity in the presence of BreR was observed at position −195 in the noncoding strand (Fig. 4A). The AB_d site contains a region of dyad symmetry that has a total of 10 mismatches and consists of 9-bp half sites separated by 6 bp (Fig. 4C, indicated by gray arrows).

The AB_p binding site was located 141 bp downstream of the AB_d site, and it extends from positions −54 to −26 and from −30 to −56 on the coding and noncoding strands, respectively (Fig. 4B). The AB_p site overlaps the −35 region, similar to the R site at the *breR* promoter (Fig. 2 and 4), and contains a region of dyad symmetry that has a total of 4 mismatches and consists of 9-bp half sites separated by 6 bp (Fig. 4C, indicated by gray arrows). These results show that the AB_p site contains the region of dyad symmetry ds11 predicted by the Vienna program (Fig. 3A), and the AB_d site contains the regions ds6 and ds7. Additionally, they suggest that BreR represses *breAB* expression by interacting with the AB_p site that overlaps the −35 region and the AB_d site located 141 bp upstream of the AB_p site.

Identification of conserved base pairs within the R, AB_p, and AB_d binding sites. To determine if a BreR recognition consensus sequence could be discerned, we compared the BreR binding sites at the *breR* and *breAB* promoters. Sequence alignment of the protected nucleotides of the coding and noncoding strands of the R, AB_p, and AB_d sites was performed using DNASTAR software. Using a cutoff of 5/6 residue identity in any given position as consensus (Fig. 5A, shaded in gray tones), an 18-bp region of dyad symmetry separated by 6 bp (AANGTANAC-N_6-GTNTACNTT) was found within the protected regions (Fig. 5A). Of these 18 bp, 6 are 100% conserved in the three binding sites (Fig. 5A, shaded in dark gray).

Mutations at the R, AB_p, and AB_d binding sites prevent BreR binding *in vitro*. The nucleotides identified in the binding site alignment that were 100% conserved (Fig. 5A, shaded in dark gray) were then mutated to investigate their importance for BreR binding at the R, AB_p, and AB_d binding sites. Two of the six conserved nucleotides were within the −35 consensus region in the *breR* and *breAB* promoters (Fig. 5A, boxed nucleotides). In order to maintain the integrity of the −35 region, mutations were only made in the conserved base pairs located in the half site upstream of the −35 site (Fig. 5A, shaded in dark gray and highlighted in boldface). The A residues at positions −50 and −44 were changed to G residues (A-50G/A-44G; named Rmut) within the *breR* promoter (Fig. 5A, shaded in dark gray and highlighted in boldface, and B, highlighted in boldface). Base pair substitutions within the *breAB* promoter were performed in the AB_p (A-52G/T-49C/A-46G; named AB_pmut) and AB_d (A-223G/T-220C/A-217G; named AB_dmut) binding sites (Fig. 5A, shaded in dark gray and highlighted in boldface, and B, highlighted in boldface). The mutations were incorporated into the wild-type R1 (−102 to +131), AB1 (−95 to +132), and AB2 (−382 to −76) fragments that BreR is capable of binding as previously determined by EMSA (17). The A-50G/A-44G changes in the R1 fragment (*breR* promoter) prevented BreR binding at both small (50 ng) and large (250 ng) amounts of BreR (Fig. 6A, lanes 5 and 6), whereas the same amounts of protein were capable of shifting the wild-type fragment (Fig. 6A, lanes 2 and 3). These results establish that the base

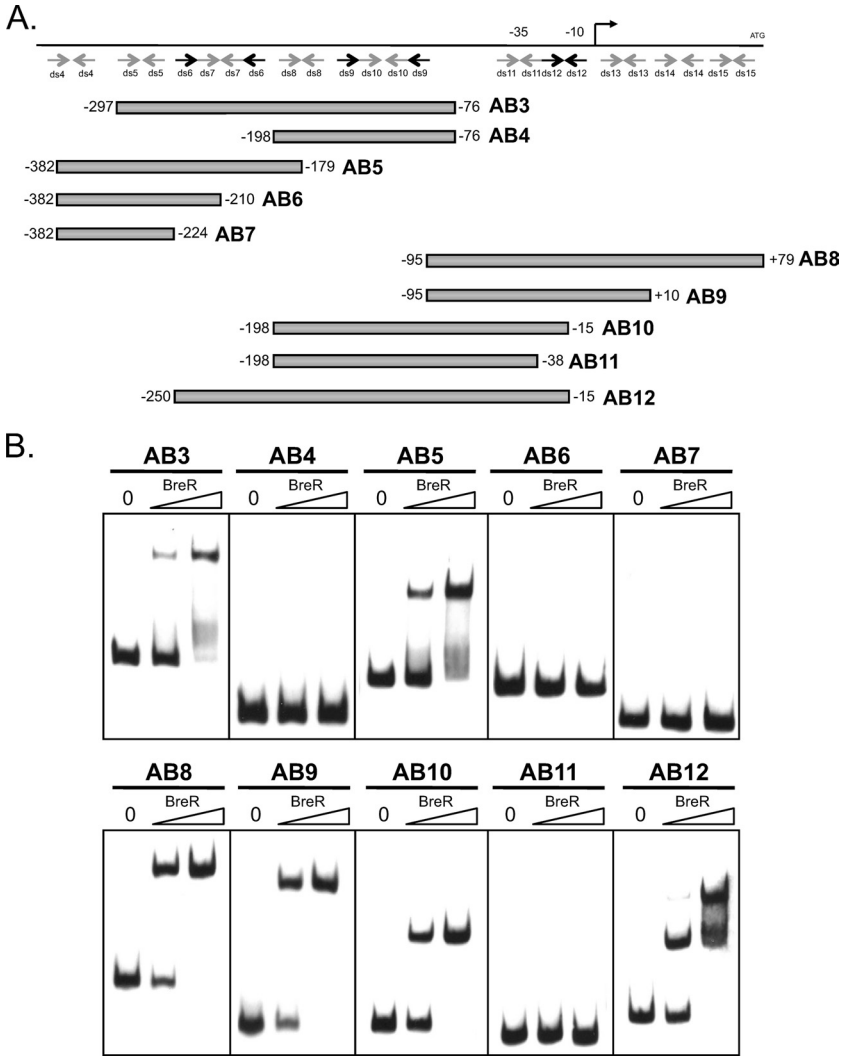

FIG 3 Mapping of the distal and proximal BreR binding sites at the *breAB* promoter region using a series of DNA fragments. (A) Schematic representation of the AB_d (−382 to −76) and AB_p (−95 to +132) fragments. Putative regions of dyad symmetry (ds4, ds5, ds6, ds7, ds8, ds9, ds10, ds11, ds12, ds13, ds14, and ds15) predicted by the Vienna program are indicated by gray or black arrows. Various DNA fragments (AB3, AB4, AB5, AB6, AB7, AB8, AB9, AB10, AB11, and AB12) used for EMSA are shown by gray boxes. The transcriptional start site is indicated by a black arrow. The ATG start codon and putative −35 and −10 regions are also shown. (B) EMSA showing BreR binding to promoter region fragments. In each panel, 10 ng DIG-dUTP-labeled DNA was incubated with 0 (first lane), 50 (second lane), or 250 ng (third lane) of BreR-His_6 prior to electrophoresis.

pair substitutions at the R site are important for BreR binding at this site *in vitro*. At the *breAB* promoter, the A-52G/T-49C/A-46G mutations in the AB_p site prevented BreR from binding to the AB1 fragment at small and large protein amounts (Fig. 7A, lanes 5 and 6) that were able to shift the wild-type AB1 fragment (Fig. 7A, lanes 2 and 3). The A-223G/T-220C/A-217G changes within the AB_d site also prevented BreR from binding to the AB2 fragment at small and large protein amounts (Fig. 7A, lanes 11 and 12), while the same amounts of BreR could bind the wild-type AB2 fragment (Fig. 7A, lanes 8 and 9). These data suggest that the mutations at the AB_p and AB_d sites are important for BreR binding *in vitro*. Further analysis of BreR binding at the wild-type AB1 and AB2 fragments indicates that 250 ng of BreR fully shifted the AB1 fragment, containing the AB_p site, compared to a partial shift of the AB2 fragment, containing the AB_d site (Fig. 7A). This is also observed with the wild-type AB3 and AB6 fragments (Fig. 2C). These results suggest that, *in vitro*, BreR affinity for the AB_d site is lower than the affinity for the AB_p site.

Mutations within the R binding site affect BreR repression of the *breR* promoter *in vivo*. To further investigate if the A-50G/A-44G changes that prevent BreR binding to the R1 fragment *in vitro* affected autoregulation *in vivo*, these mutations were introduced into a P_{breR}-*lacZ* transcriptional fusion. BreR repression of the *breR* promoter was assessed in wild-type and Δ*breR* strains harboring a P_{breR}-*lacZ* fusion at the *lacZ* locus carrying the wild-type or mutated promoters. It has previously been reported that expression of *breR* is induced in response to bile and that deletion of BreR increases P_{breR}-*lacZ* expression in the absence and presence of bile compared to the response of the wild type, suggesting that expression of *breR* is obtained by BreR derepression (17). Similarly, the mutations that disrupt BreR binding also caused derepression of P_{breR}-*lacZ* in the absence and presence of bile. The

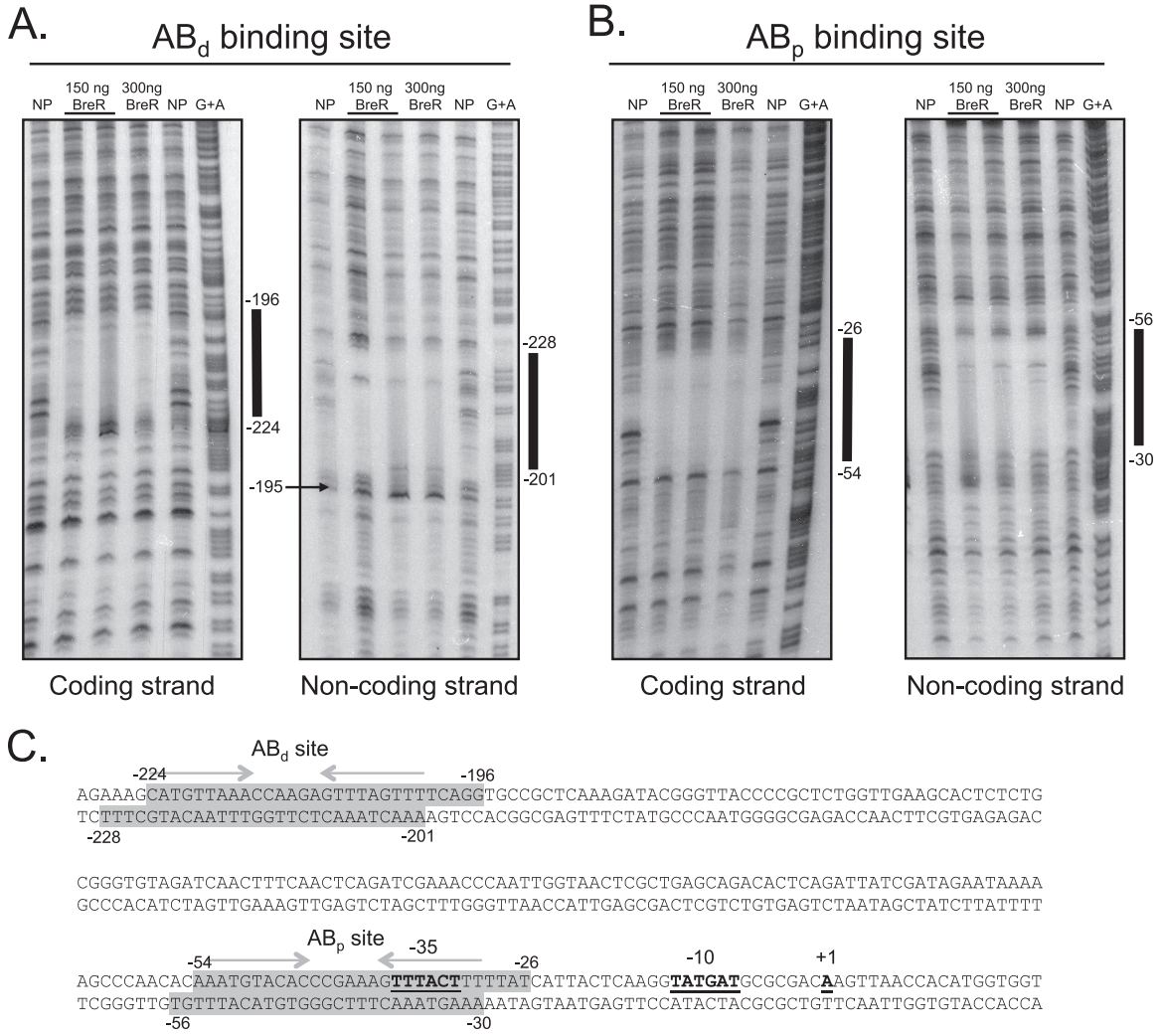

FIG 4 DNase I footprinting analyses for BreR at the *breAB* promoter. The coding and noncoding strands of two radioactively ^{33}P-end-labeled fragments of 230 bp (−327 to −97) (A) and 246 bp (−167 to +78) (B) were incubated with a 1:200 dilution of DNase I and no protein (NP; lanes 1 and 5), ~150 ng BreR and a 1:200 DNase I dilution (lane 2) or a 1:400 DNase I dilution (lane 3), ~300 ng BreR and a 1:200 dilution of DNase I (lane 4), and a G+A sequencing reaction (lane 6). The region of protection by BreR and a region of hypersensitivity induced by BreR are indicated by thick black lines and a black arrow, respectively. (C) Double-stranded DNA sequence of the *breAB* promoter. BreR-protected regions are shaded in gray for both strands. Regions of partial dyad symmetry, involved in DNA binding, are shown for the AB$_d$ and AB$_p$ binding sites with gray arrows. The transcriptional start site (+1) (17), ATG start codon, and putative −35 and −10 regions are highlighted in boldface and are underlined.

A-50G/A-44G mutations increased P$_{breR}$-*lacZ* expression 9.5- and 2-fold in the absence and presence of bile, respectively, compared to the wild type (Fig. 6B). Deletion of *breR* in the presence of these mutations did not further derepress P$_{breR}$-*lacZ* expression, suggesting that these mutations cause a loss of BreR repression. This expression was not as high as that of the *breR* mutation, suggesting that these mutations alter basal expression by RNA polymerase. These data establish that repression of *breR* expression results from BreR binding to the R binding site (region from −50 to −24), and that conserved nucleotides A-50, A-44, or both are essential for BreR repression.

Mutations only in the AB$_p$ binding site affect BreR binding to the *breAB* promoter *in vivo*. To determine if the mutations affecting BreR binding to the AB$_p$ and AB$_d$ sites *in vitro* alter BreR repression of *breAB in vivo*, the A-52G/T-49C/A-46G and -223G/T-220C/A-217G mutations were introduced into a P$_{breAB}$-*lacZ* transcriptional fusion. The influence of the mutations on BreR-mediated repression of *breAB* expression was determined using wild-type and Δ*breR* strains harboring P$_{breAB}$-*lacZ* fusions carrying the wild-type or mutated promoters. As shown previously (17), Fig. 7B confirms that P$_{breAB}$-*lacZ* expression is higher in the presence of bile and that deletion of *breR* causes increased P$_{breAB}$-*lacZ* expression in the absence and presence of bile. Expression from the fusion containing the substitutions at the AB$_p$ region (A-52G/T-49C/A-46G [AB$_p$mut]) showed a 19.7-fold increase in the absence of bile and a 1.8-fold increase in the presence of bile compared to the wild type, indicating a critical role for the AB$_p$ binding site *in vivo* (Fig. 7B). Introduction of the *breR* mutation into this background did not further derepress P$_{breAB}$-*lacZ* expression, suggesting that the mutations in the AB$_p$ site cause a loss of BreR repression (Fig. 7B). The mutations at the AB$_p$ site did not increase P$_{breAB}$-*lacZ* expression to the levels observed in the Δ*breR*

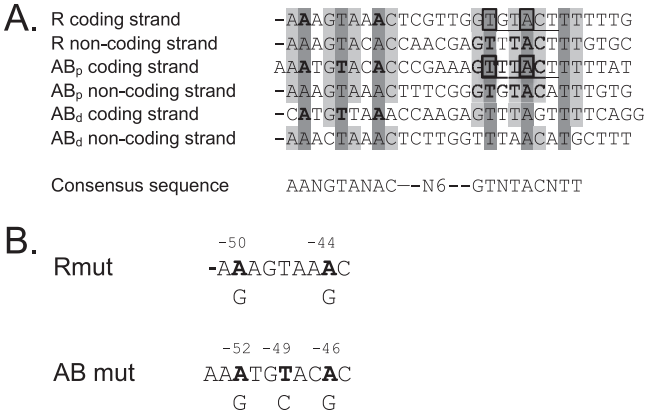

FIG 5 BreR binding consensus sequence. (A) Sequence alignment of the coding and noncoding strands of the R, AB_p, and AB_d binding sites. Conserved base pairs are shaded in gray tones. Base pairs selected for substitution are shaded in dark gray and are highlighted in boldface. The −35 regions at the R and AB_p sites are underlined, and the consensus region is also shown. Boxes indicate conserved nucleotides within the −35 region of the R and AB promoters. (B) Schematic representation of the bases selected for substitutions (A-50 and A-44 in the R site, A-52, T-49, and A-46 in the AB_p site, and A-223, T-220, and A-217 in the AB_d site). Each mutated base is in boldface. The position number is shown above, and the base to which it was changed is shown below.

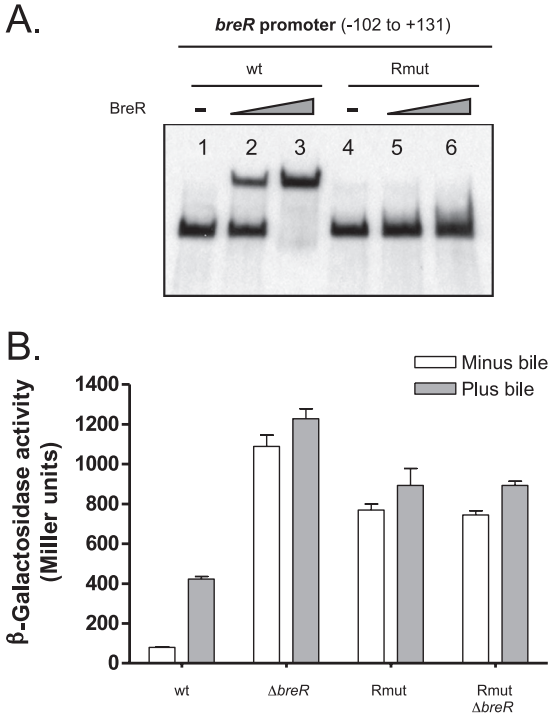

FIG 6 Mutational analysis of the R binding site at the *breR* promoter. (A) BreR binding to the wild-type and mutated (Rmut) R1 fragment. EMSA was performed using DIG-dUTP-labeled DNA (10 ng) incubated with 0 (lanes 1 and 4), 50 (lanes 2 and 5), or 250 ng (lanes 3 and 6) of BreR-His_6 prior to electrophoresis. (B) Expression of the P_{breR}-*lacZ* fusion carrying the wild-type or mutated promoter in different strain backgrounds. β-Galactosidase activity was measured by growing the strains in the absence or presence of 0.4% bile in LB at 37°C until the optical density at 600 nm of the cultures had reached 0.8 to 1.0. Results are from three independent experiments. Error bars indicate standard deviations.

strain, suggesting that these mutations alter basal expression. Expression from the P_{breAB}-*lacZ* fusion containing the mutations in the AB_d region (A-223G/T-220C/A-217G [AB_dmut]) in the wild-type and Δ*breR* backgrounds was similar to that of the wild-type promoter *lacZ* fusion grown with or without bile in the wild-type and Δ*breR* strains (Fig. 7B). These results suggest that disruption of BreR binding at this site does not influence the repression of P_{breAB}-*lacZ* expression by BreR *in vivo*. A P_{breAB}-*lacZ* fusion containing mutations at both the AB_p and AB_d regions was also defective for binding, and *lacZ* expression was similar to that obtained with the promoter *lacZ* fusion carrying the mutations in the AB_p site (Fig. 7B). These results indicate that BreR represses *breAB* expression *in vivo* by binding exclusively to the AB_p binding site (region from −54 to −26), and that binding at this region can be disrupted by a 3-bp change at positions −52, −49, and −46.

Deletion of *breR* does not affect colonization in the infant mouse model. It has previously been shown that in the absence of BreR, the *breAB* genes are overexpressed (17) and there is more resistance to cholate when this strain is grown in liquid media compared to that of the wild type (data not shown). To determine if BreR plays a role in an *in vivo* infection model, the Δ*breR* mutant was competed against a wild-type strain in the infant mouse colonization model. The Δ*breR* mutant was not reduced in colonization compared to the wild type (data not shown). These results indicate that BreR does not play a role in intestinal colonization in this model, and this may be attributed to the fact that the infant mouse does not produce bile.

DISCUSSION

The TetR regulator, BreR, and the efflux system BreAB have been identified as being important in the response of *V. cholerae* to bile (17). The work presented here begins to define the regulatory mechanisms employed by BreR to regulate the expression of the *breR* gene and the *breAB* operon.

Since most of the TetR family regulators bind to their binding sites (complete or partial regions of dyad symmetry) as dimers (32), we initially searched for regions of dyad symmetry present at the *breR* and *breAB* promoters using a program that predicts RNA secondary structures. EMSA studies using these predictions followed by DNase I footprinting showed that BreR binds at the *breR* promoter (R binding site) at a unique region from position −55 to −24 and binds to the *breAB* promoter at two independent sites, a proximal site (AB_p) located at −56 to −26 and a distal site (AB_d) located at −228 to −196. A DNase I hypersensitive site was induced by BreR at the AB_d binding site (Fig. 4A), indicating a change in DNA conformation upon BreR binding. When the coding and noncoding sequences of these binding sites were aligned, the analysis revealed that BreR recognizes the consensus sequence AANGTANAC-N_6-GTNTACNTT. This sequence contains 18 conserved base pairs that are symmetrical, suggesting that BreR binds as a homodimer, as has been shown for other TetR family repressors (32).

In order to genetically determine if the consensus site defined requirements for BreR binding, substitutions were performed on consensus base pairs that were 100% conserved. Introduction of the A-50G/A-44G base pair mutations into the *breR* promoter completely abolished BreR binding to the *breR* promoter and prevented transcriptional repression by BreR. These data established that BreR binds the *breR* promoter region at a position that over-

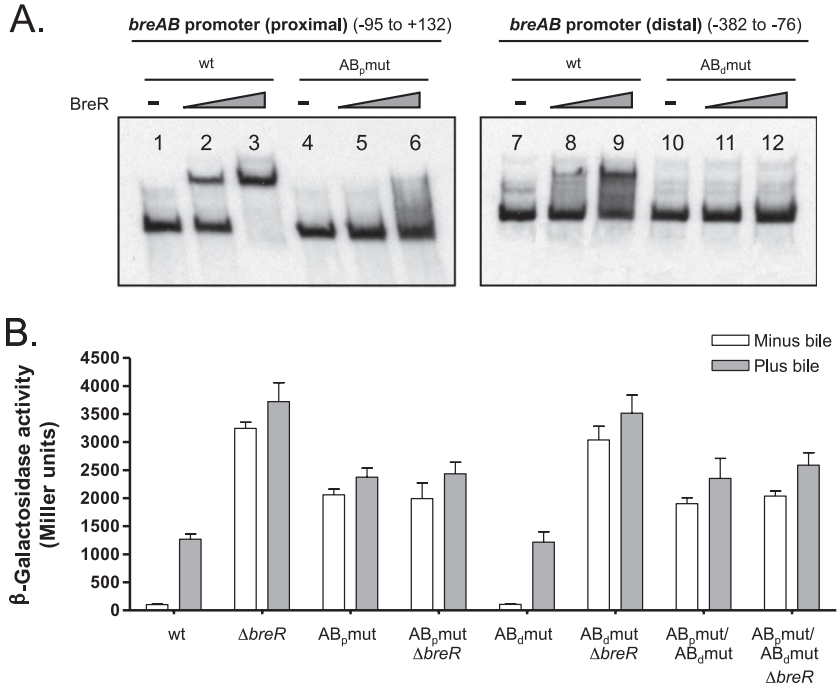

FIG 7 Mutational analysis of the AB_p and AB_d binding sites at the *breAB* promoter. (A) Binding of BreR to the wild-type and mutated (AB_pmut and AB_dmut) AB_p and AB_d fragments. EMSA was performed using DIG-dUTP-labeled DNA (10 ng) incubated with 0 (lanes 1, 4, 7, and 10), 50 (lanes 2, 5, 8, and 11), or 250 ng (lanes 3, 6, 9, and 12) of BreR-His_6 prior to electrophoresis. (B) Influence of base pair mutations in P_{breAB}-*lacZ* expression in various strain backgrounds. β-Galactosidase activity was measured as described for Fig. 6.

laps the −35 consensus site. Mutations at the AB_p site (A-52G/T-49C/A-46G) inhibited BreR binding to this site and eliminated repression at the *breAB* promoter. The base pair changes at the AB_d site (A-223G/T-220C/A-217G) prevented BreR binding to AB_d; however, they did not prevent *breAB* transcriptional repression by BreR, suggesting that the AB_d site does not play a key role in BreR repression *in vivo*. A possible explanation for why the AB_d site did not show a role *in vivo* is based on the position of this site. The AB_d site is located 158 bp upstream of the −35 consensus region, suggesting that although BreR can bind to the AB_d site, it is excessively distant in order to interfere with RNA polymerase binding. Another explanation could be based on the sequence of the AB_d binding site. While the R and AB_p sites display a high degree of sequence similarity to the BreR consensus sequence (Fig. 5), the AB_d site exhibits four mismatches (Fig. 5). This observation suggests that even though BreR can bind to the AB_d site *in vitro*, this interaction is of low affinity compared to those of the other BreR binding sites. This is supported by the fact that 250 ng of BreR protein completely shifted the wild-type AB1 fragment (−95 to +132) compared to a lower percentage of shift for the wild-type AB2 fragment (−382 to −76) (Fig. 7A) (17). Overall, it appears that BreR represses *breAB* expression by binding at a single site (AB_p) in the *breAB* promoter that overlaps the −35 region. Moreover, the mutations generated at the R and AB_p sites abolish BreR binding (Fig. 2B and 4C), suggesting that these base pairs play an important role in BreR binding.

Double or triple mutations in the dyad symmetry of the R and AB_p binding sites in the wild-type and Δ*breR* backgrounds significantly reduced the level of BreR binding, resulting in overexpression of the mutated P_{breR}-*lacZ* and P_{breAB}-*lacZ* fusions *in vivo*. However, overexpression from these promoters was not as high as the overexpression from the Δ*breR* strain harboring either P_{breR}-*lacZ* or P_{breAB}-*lacZ* wild-type *lacZ* transcriptional fusions (Fig. 6B and 7B). A partial overexpression could be attributed to the fact that the mutations were localized 9 to 15 bp upstream of the −35 region, and they could affect expression by influencing RNA polymerase interaction with the DNA or alter the binding site of an unknown activator. Another possible explanation arises when comparing the shift of the Rmut and AB_pmut fragments induced by addition of large amounts of BreR (250 ng) (Fig. 6A and 7A). The comparison shows that there is a slight but detectable shift with both mutated probes in the presence of 250 ng of BreR, suggesting that the mutations do not abolish BreR binding completely. This also could take place *in vivo*, explaining the expression levels of the mutated P_{breR}-*lacZ* and P_{breAB}-*lacZ* (Fig. 6A and 7A).

A number of TetR regulators, such as VceR (33, 34), CmeR (22), MexL (35), MexZ (36), TtgV (37), LmrA (25), TtgR (38), QacR (39), MtrR (40), and TcmR (41), also repress the expression of genes encoding efflux pumps by binding to complete or partial regions of dyad symmetry within the promoter region of their target genes (18, 32). Some of the operator sequences overlap both the −35 and −10 consensus sites (35–38, 40, 41), whereas others overlap only the −10 (25, 33, 39) or the −35 region (22), indicating that they most probably block RNA polymerase binding. The location of the R and AB_p binding sites, overlapping the −35 region at the *breR* and *breAB* promoters, respectively, is consistent with the role of BreR as a negative regulator and shows a binding pattern shared by other TetR repressors. It is most likely that BreR

inhibits initiation of transcription by physically preventing RNA polymerase access to the *breR* and *breAB* promoter region.

Since the expression of *breR* and *breAB* is controlled by bile, we propose the following regulation model. In the absence of bile, BreR binds to the consensus sequence AANGTANAC-N_6-GTNT ACNTT overlapping the −35 region of the *breR* and *breAB* promoters. As a result, BreR inhibits initiation of transcription by blocking RNA polymerase binding and maybe binding of an activator. In the presence of bile, *V. cholerae* has to be able to resist its bactericidal effect, therefore it utilizes bile as a signal to turn on the *breAB* resistance genes. In addition, *breR* expression is also turned on to tightly control *breAB* expression to prevent extrusion of vital cellular metabolites and loss of membrane potential. We have previously proposed that certain bile salts (cholate, deoxycholate, and/or glycodeoxycholate) bind BreR, inducing a conformational change that disrupts its interaction with DNA (17), identified here as the R and AB_p binding sites. As a consequence, expression of *breAB* takes place and the toxic compounds are extruded out of the cell, upon which BreR is available to rapidly repress *breAB* gene expression and prevent further extrusion of critical metabolites or loss of membrane potential.

ACKNOWLEDGMENTS

We thank Emily Stonehouse for helpful discussions and critical reading of the manuscript.

This work was supported by NIH grant AI039654 and NSF grant OCN-0120677.

REFERENCES

1. **Champion GA, Neely MN, Brennan MA, DiRita VJ.** 1997. A branch in the ToxR regulatory cascade of *Vibrio cholerae* revealed by characterization of *toxT* mutant strains. Mol. Microbiol. **23**:323–331.
2. **Withey JH, DiRita VJ.** 2006. The toxbox: specific DNA sequence requirements for activation of *Vibrio cholerae* virulence genes by ToxT. Mol. Microbiol. **59**:1779–1789.
3. **Kovacikova G, Skorupski K.** 1999. A *Vibrio cholerae* LysR homolog, AphB, cooperates with AphA at the *tcpPH* promoter to activate expression of the ToxR virulence cascade. J. Bacteriol. **181**:4250–4256.
4. **Matson JS, Withey JH, DiRita VJ.** 2007. Regulatory networks controlling *Vibrio cholerae* virulence gene expression. Infect. Immun. **75**:5542–5549.
5. **Begley M, Gahan CG, Hill C.** 2005. The interaction between bacteria and bile. FEMS Microbiol. Rev. **29**:625–651.
6. **Hofmann AF.** 1998. Bile secretion and the enterohepatic circulation of bile salts, 6th ed. W. B. Saunders, Philadelphia, PA.
7. **Gunn JS.** 2000. Mechanisms of bacterial resistance and response to bile. Microbes Infect. **2**:907–913.
8. **Gupta S, Chowdhury R.** 1997. Bile affects production of virulence factors and motility of *Vibrio cholerae.* Infect. Immun. **65**:1131–1134.
9. **Schuhmacher DA, Klose KE.** 1999. Environmental signals modulate ToxT-dependent virulence factor expression in *Vibrio cholerae.* J. Bacteriol. **181**:1508–1514.
10. **Hung DT, Zhu J, Sturtevant D, Mekalanos JJ.** 2006. Bile acids stimulate biofilm formation in *Vibrio cholerae.* Mol. Microbiol. **59**:193–201.
11. **Bina JE, Provenzano D, Wang C, Bina XR, Mekalanos JJ.** 2006. Characterization of the *Vibrio cholerae vexAB* and *vexCD* efflux systems. Arch. Microbiol. **186**:171–181.
12. **Provenzano D, Klose KE.** 2000. Altered expression of the ToxR-regulated porins OmpU and OmpT diminishes *Vibrio cholerae* bile resistance, virulence factor expression, and intestinal colonization. Proc. Natl. Acad. Sci. U. S. A. **97**:10220–10224.
13. **Provenzano D, Schuhmacher DA, Barker JL, Klose KE.** 2000. The virulence regulatory protein ToxR mediates enhanced bile resistance in *Vibrio cholerae* and other pathogenic *Vibrio* species. Infect. Immun. **68**:1491–1497.
14. **Chatterjee A, Chaudhuri S, Saha G, Gupta S, Chowdhury R.** 2004. Effect of bile on the cell surface permeability barrier and efflux system of *Vibrio cholerae.* J. Bacteriol. **186**:6809–6814.
15. **Bina JE, Mekalanos JJ.** 2001. *Vibrio cholerae tolC* is required for bile resistance and colonization. Infect. Immun. **69**:4681–4685.
16. **Colmer JA, Fralick JA, Hamood AN.** 1998. Isolation and characterization of a putative multidrug resistance pump from *Vibrio cholerae.* Mol. Microbiol. **27**:63–72.
17. **Cerda-Maira FA, Ringelberg CS, Taylor RK.** 2008. The bile response repressor BreR regulates expression of the *Vibrio cholerae breAB* efflux system operon. J. Bacteriol. **190**:7441–7452.
18. **Grkovic S, Brown MH, Skurray RA.** 2002. Regulation of bacterial drug export systems. Microbiol. Mol. Biol. Rev. **66**:671–701.
19. **Li XZ, Nikaido H.** 2004. Efflux-mediated drug resistance in bacteria. Drugs **64**:159–204.
20. **Aires JR, Kohler T, Nikaido H, Plesiat P.** 1999. Involvement of an active efflux system in the natural resistance of *Pseudomonas aeruginosa* to aminoglycosides. Antimicrob. Agents Chemother. **43**:2624–2628.
21. **Hagman KE, Shafer WM.** 1995. Transcriptional control of the *mtr* efflux system of *Neisseria gonorrhoeae.* J. Bacteriol. **177**:4162–4165.
22. **Lin J, Akiba M, Sahin O, Zhang Q.** 2005. CmeR functions as a transcriptional repressor for the multidrug efflux pump CmeABC in *Campylobacter jejuni.* Antimicrob. Agents Chemother. **49**:1067–1075.
23. **Ma D, Alberti M, Lynch C, Nikaido H, Hearst JE.** 1996. The local repressor AcrR plays a modulating role in the regulation of *acrAB* genes of *Escherichia coli* by global stress signals. Mol. Microbiol. **19**:101–112.
24. **Namwat W, Lee CK, Kinoshita H, Yamada Y, Nihira T.** 2001. Identification of the *varR* gene as a transcriptional regulator of virginiamycin S resistance in *Streptomyces virginiae.* J. Bacteriol. **183**:2025–2031.
25. **Yoshida K, Ohki YH, Murata M, Kinehara M, Matsuoka H, Satomura T, Ohki R, Kumano M, Yamane K, Fujita Y.** 2004. *Bacillus subtilis* LmrA is a repressor of the *lmrAB* and *yxaGH* operons: identification of its binding site and functional analysis of *lmrB* and *yxaGH.* J. Bacteriol. **186**:5640–5648.
26. **Miller JH.** 1972. Experiments in molecular genetics. Cold Spring Harbor Laboratory Press, Cold Spring Harbor, NY.
27. **Kovacikova G, Skorupski K.** 2002. Regulation of virulence gene expression in *Vibrio cholerae* by quorum sensing: HapR functions at the *aphA* promoter. Mol. Microbiol. **46**:1135–1147.
28. **Skorupski K, Taylor RK.** 1996. Positive selection vectors for allelic exchange. Gene **169**:47–52.
29. **Kovacikova G, Skorupski K.** 2001. Overlapping binding sites for the virulence gene regulators AphA, AphB and cAMP-CRP at the *Vibrio cholerae tcpPH* promoter. Mol. Microbiol. **41**:393–407.
30. **Kovacikova G, Lin W, Skorupski K.** 2005. Dual regulation of genes involved in acetoin biosynthesis and motility/biofilm formation by the virulence activator AphA and the acetate-responsive LysR-type regulator AlsR in *Vibrio cholerae.* Mol. Microbiol. **57**:420–433.
31. **Taylor RK, Miller VL, Furlong DB, Mekalanos JJ.** 1987. Use of *phoA* gene fusions to identify a pilus colonization factor coordinately regulated with cholera toxin. Proc. Natl. Acad. Sci. U. S. A. **84**:2833–2837.
32. **Ramos JL, Martinez-Bueno M, Molina-Henares AJ, Teran W, Watanabe K, Zhang X, Gallegos MT, Brennan R, Tobes R.** 2005. The TetR family of transcriptional repressors. Microbiol. Mol. Biol. Rev. **69**:326–356.
33. **Alatoom AA, Aburto R, Hamood AN, Colmer-Hamood JA.** 2007. VceR negatively regulates the *vceCAB* MDR efflux operon and positively regulates its own synthesis in *Vibrio cholerae* 569B. Can. J. Microbiol. **53**:888–900.
34. **Borges-Walmsley MI, Du D, McKeegan KS, Sharples GJ, Walmsley AR.** 2005. VceR regulates the *vceCAB* drug efflux pump operon of *Vibrio cholerae* by alternating between mutually exclusive conformations that bind either drugs or promoter DNA. J. Mol. Biol. **349**:387–400.
35. **Chuanchuen R, Gaynor JB, Karkhoff-Schweizer R, Schweizer HP.** 2005. Molecular characterization of MexL, the transcriptional repressor of the *mexJK* multidrug efflux operon in *Pseudomonas aeruginosa.* Antimicrob. Agents Chemother. **49**:1844–1851.
36. **Matsuo Y, Eda S, Gotoh N, Yoshihara E, Nakae T.** 2004. MexZ-mediated regulation of *mexXY* multidrug efflux pump expression in *Pseudomonas aeruginosa* by binding on the *mexZ-mexX* intergenic DNA. FEMS Microbiol. Lett. **238**:23–28.
37. **Rojas A, Segura A, Guazzaroni ME, Teran W, Hurtado A, Gallegos MT, Ramos JL.** 2003. *In vivo* and *in vitro* evidence that TtgV is the specific regulator of the TtgGHI multidrug and solvent efflux pump of *Pseudomonas putida.* J. Bacteriol. **185**:4755–4763.

38. **Teran W, Felipe A, Segura A, Rojas A, Ramos JL, Gallegos MT.** 2003. Antibiotic-dependent induction of *Pseudomonas putida* DOT-T1E TtgABC efflux pump is mediated by the drug binding repressor TtgR. Antimicrob. Agents Chemother. **47**:3067–3072.
39. **Grkovic S, Brown MH, Roberts NJ, Paulsen IT, Skurray RA.** 1998. QacR is a repressor protein that regulates expression of the *Staphylococcus aureus* multidrug efflux pump QacA. J. Biol. Chem. **273**:18665–18673.
40. **Lucas CE, Balthazar JT, Hagman KE, Shafer WM.** 1997. The MtrR repressor binds the DNA sequence between the *mtrR* and *mtrC* genes of Neisseria gonorrhoeae. J. Bacteriol. **179**:4123–4128.
41. **Guilfoile PG, Hutchinson CR.** 1992. The Streptomyces glaucescens TcmR protein represses transcription of the divergently oriented *tcmR* and *tcmA* genes by binding to an intergenic operator region. J. Bacteriol. **174**:3659–3666.